

NONLINEAR POLARIZATION SPECTROSCOPY (FREQUENCY DOMAIN) STUDIES OF EXCITED STATE PROCESSES: THE B800–850 ANTENNA OF *RHODOBACTER SPHAEROIDES*

DIETER LEUPOLD*¹, BERND VOIGT¹, MICHAEL PFEIFFER¹,
MICHAEL BANDILLA² and HUGO SCHEER²

¹Max-Born Institut für Nichtlineare Optik und Kurzzeitspektroskopie, Rudower Chaussee 6, D-O-1199 Berlin, Germany, and
²Botanisches Institut der Universität München, Menzinger Straße 67, D-W-8000 München 19, Germany

(Received 6 April 1992; Accepted 21 July 1992)

Abstract—Nonlinear polarization spectroscopy in the frequency domain allows rate constant determinations of fast electronic energy and phase relaxations together with characterization of the type of line broadening. Application of this method to the B850 component of the isolated B800–850 antenna of *Rhodobacter sphaeroides* at room temperature shows that B850 is inhomogeneously broadened, with homogeneous widths between 30 and 200 cm⁻¹, depending on the spectral position of the subforms. The corresponding phase relaxation times are clearly in the subpicosecond range. There is also indication of an up-to-now unspecified 1–5 ps energy relaxation channel per subunit.

INTRODUCTION

The light-harvesting antenna of *Rhodobacter sphaeroides* consists of two functional parts: The core complex LH I, called also B875 according to the longest wavelength absorption maximum of its complex-bound bacteriochlorophyll *a* (BChl),† and the peripheral part LH II, also characterized as B800–850 according to the maxima of the two BChl *a* components contained.

The ultrafast processes realizing the efficient light harvesting in LH II were intensively studied during the last decade with the complete photosynthetic apparatus in chromatophores as well as with the isolated B800–850 complex, and with a special mutant containing only LH II. (For comprehensive overview see Scheer and Schneider,¹ and Scheer.²)

Recent investigations have concentrated on the apparent spectral heterogeneity of the BChl 850 absorption band, *e.g.*, on the role of a minor component absorbing at 870 nm. This compound was found in the LH II-containing mutant NF 57 and also indicated in membranes of *Rhodobacter sphaeroides*, but not in the isolated B800–850 complex.³ Heterogeneity of this band is also indicated by different pathways of energy transfer from the short and long wave length wings of the BChl 850 band to LH I,^{4,5} as well as by two types of exciton annihilation found within BChl 850.⁶ On the other hand, low-temperature hole-burning investigations indicate homogeneous broadening of BChl 850.⁷

An additional point of more general interest to all photosynthetic antennas has come into discussion by recent studies on picosecond phase relaxation times T_2 at room temperature. Theoretical⁸ as well as experimental^{9,10} arguments for values of T_2 as long as several picoseconds were published, especially with photosystem II membrane fragments (BBY particles).¹¹ This is rather unexpected and conflicts with the

usual (incoherent) approach to model the complex picosecond excited state kinetics in antennas.

In the following, first results will be presented on phase relaxation times in B800–850 at room temperature, obtained by the method of nonlinear polarization spectroscopy in the frequency domain (NLPF). The values are clearly in the subpicosecond range.‡ NLPF signals are also well suited to give insight to band broadening and spectral heterogeneity. The measurements, concentrated up to now on the BChl 850 absorption band of the isolated B800–850 complex, show inhomogeneous broadening, *i.e.*, the B850 component has a detailed substructure. The homogeneous widths of the subforms depend on their spectral position within the B850 absorption band.

MATERIALS AND METHODS

Antenna-complex B800–850

Chromatophores (OD₈₅₀ = 50 cm⁻¹) of *Rb. sphaeroides* 2.4.1. (ATCC 17023)¹² were solubilized in Tris/HCl buffer (10 mM, pH 8.0) containing 2% vol/vol Triton-BG 10 (Röhm und Haas). After centrifugation (1 h at 240 000 g) the supernatant was chromatographed repeatedly on DEAE-cellulose (DE52 Whatman/solubilization buffer with only 0.2% vol/vol Triton BG 10, 50–500 mM NaCl gradient) until the 880 nm shoulder and the shoulder in the region between 745 to 780 nm had disappeared, and in the sodium dodecyl sulfate polyacrylamide gel electrophoresis (SDS-PAGE) (Laemmli,¹³ using gradient gels of 10%/3% cross-linker to 18%/6% cross-linker) no reaction-center polypeptides were detectable. The B800–850 antenna eluted as the last fraction at about 200 mM NaCl. For storage the antenna was dialyzed against Tris/HCl (20 mM, pH 8). Before the measurements, the antenna was redissolved in LDAO (*N,N*-dimethyldodecylamine-*N*-oxide) buffer (Tris/HCl [10 mM, pH 8.0] containing 0.1% vol/vol LDAO), equilibrated by five to six times of freeze–thaw cycles, chromatographed on DEAE-cellulose using LDAO buffer (0–500 mM NaCl gradient) and dialyzed against LDAO buffer.

For the NLPF measurements, samples with OD₈₅₀ = 20 were used in 0.1 cm sample cells.

*To whom correspondence should be addressed.

†Abbreviations: BChl, bacteriochlorophyll *a*; FWHM, full width at half of maximum; LDAO, *N,N*-dimethyldodecylamine-*N*-oxide; NLPF, nonlinear polarization spectroscopy in the frequency domain.

‡A similar result was obtained with BBY particles at room temperature by using the NLPF method with probing at 680 nm (D. Leupold *et al.*, unpublished data). BBY samples were kindly provided by Prof. G. Renger (TU Berlin).

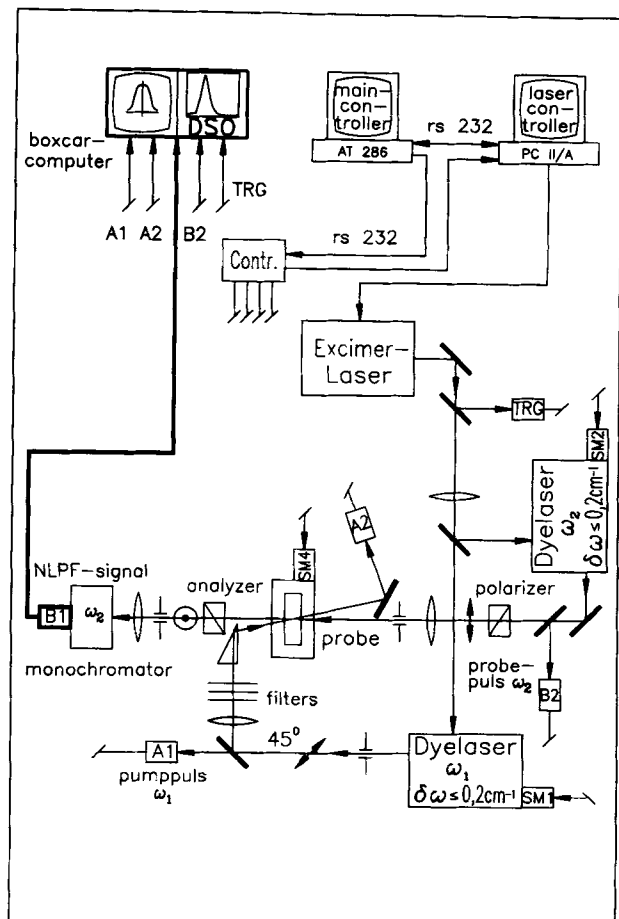


Figure 1. Experimental setup for NLPF measurements. A1, A2, B1, B2: receivers (photodiode/preamplifier); SM1, SM2: step motors (dye laser tuning); SM4: step motor (sample cell movement); DSO: digital storage oscilloscope (PM 3323, Philips); TRG: trigger.

Nonlinear polarization spectroscopy: Principle and experimental set-up

Nonlinear polarization spectroscopy in the frequency domain was introduced to condensed phase investigations of organic compounds by Song *et al.*¹⁴ Birefringence and dichroism in the sample under study are created by a linearly polarized pump wave (frequency ω_1). The sample is located between crossed polarizers and probed by a second wave (ω_2) linearly polarized at 45° to the pump wave. The signal behind the analyzer is the result of nonlinear interaction of both waves, which produces a polarization component at ω_2 that is orthogonal to the original probe wave polarization.

In our experimental setup (*cf.* Fig. 1 and legend to this figure for technical details) the intensity of this new component is measured under stationary conditions as a function of the frequency difference to the variable pump wave. After it passes a monochromator, it is detected by a photodiode–preamplifier system and a combination of a digital sampling oscilloscope and a boxcar system. Both pump and probe waves are realized by homemade grazing incidence dye lasers, simultaneously pumped by an excimer laser. The pulse width (full width at half of maximum) is 15 ns, their spectral width is $\leq 0.2 \text{ cm}^{-1}$. For the investigations around 850 nm a solution of the dye styryl 9 serves as laser material; the useful tuning range is 810–870 nm.

The NLPF measurements were generally made by a pump-to-probe intensity ratio of about 50. The photonflux density of the pump pulse was usually around $5 \times 10^{23} \text{ cm}^{-2} \text{ s}^{-1}$; variations up to one order of magnitude in both directions were used in case of intensity-dependent measurements.

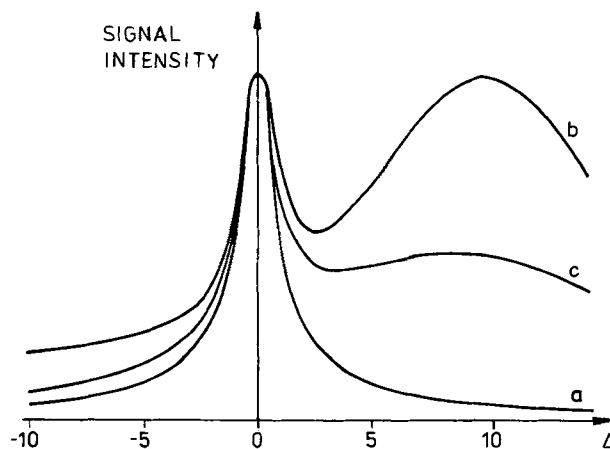


Figure 2. Schematic representation of theoretic NLPF lineshapes. a: Extremely inhomogeneously broadened electronic transition. b: Purely homogeneously broadened electronic transition. c: Example of an intermediate case.

Sample cells of 0.1 cm path length were used; the minimum diameter of the interaction volume was 0.015 cm. With a pulse repetition frequency of 2 Hz, after each pulse the cell was moved perpendicular to the probe pulse propagation by a step motor. Under these conditions the photochemical stability of the B800–850 sample was found to be excellent if judged by absorption spectroscopy. Simultaneously with the NLPF signal, pump and probe powers before and pump power behind the sample were measured. There is also continuous control of wavelength calibration, based on the optical galvanic effect, as well as Fabry-Perot control of the spectral width. All measurements were made at room temperature.

Theoretical approach

Extraction of the information contained in the measured NLPF signal requires fitting to an adequate lineshape function, which is obtained by solving the equations of motion for the density matrix describing the sample under study.^{14,15} Though an adequate model especially in case of photosynthetic objects needs inclusion of processes like energy transfer, thermal equilibration, spectral diffusion as well as excited state absorption and exciton annihilation, the main properties and general features of the NLPF signal can already be modeled with simple two level systems (with resonance frequency, ω_0 , and longitudinal [T_1] and transverse [T_2] relaxations). The inhomogeneous broadening can be taken into account by integration over ω_0 with a proper distribution function $g(\omega_0)$.¹⁶ In the case of extremely inhomogeneous broadening§ the lineshape function, *i.e.*, the NLPF signal as a function of $\Delta\omega = \omega_1 - \omega_2$, is a symmetric function with maximum at $\Delta\omega = 0$ (*cf.* Fig. 2a). The half width of the function is mainly determined by T_1 , the shape of the wings mainly by T_2 . It is noteworthy that in this case of extremely inhomogeneous broadening the shape of the signal has no relation to the maximum of the distribution, *i.e.*, it parallels by no means the overall absorption band.

In the opposite case of pure homogeneous broadening, the NLPF signal has two maxima, one again when the tuned pump frequency ω_1 coincides with the fixed probe frequency ω_2 , the other when it coincides with the maximum of the homogeneous band (*cf.* Fig. 2b). The shape shown in Fig. 2b corresponds to an ω_2 at the low frequency part of the absorption band, it is mirrored at the ordinate for ω_2 higher in frequency than the band maximum.

The transition between pure homogeneity and extremely inhomogeneous broadening can be described by a variation of the width of the distribution function. One resulting NLPF shape of an inter-

§Extremely inhomogeneous broadening means that the distribution function $g(\omega_0)$ is constant within the homogeneous width (homogeneous width \ll bandwidth of absorption band).

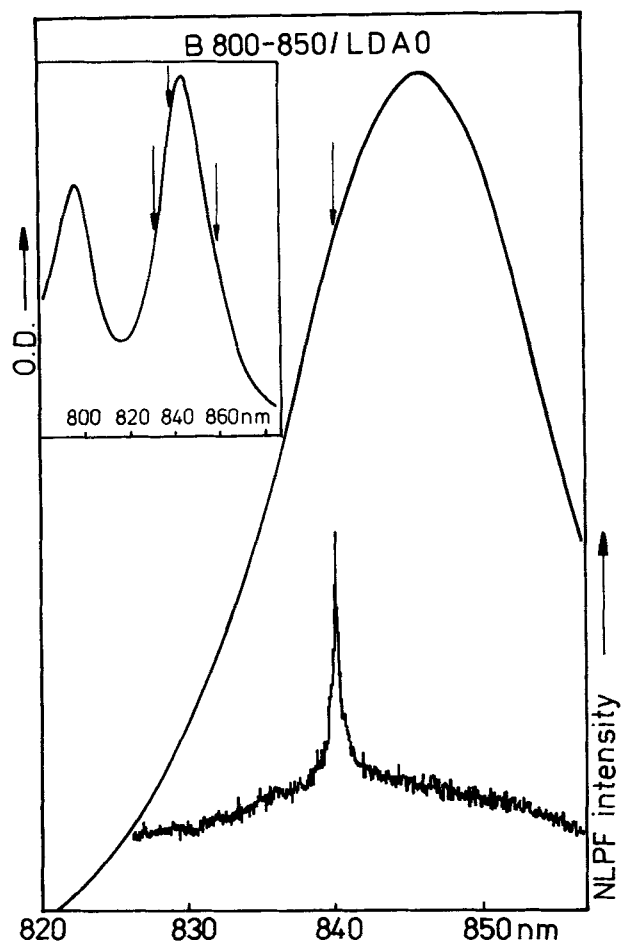


Figure 3. Upper left part: Absorption spectrum of the B800–850 complex in Tris-HCl buffer (10 mM, pH 8) containing 0.1% LDAO. Arrows indicate probe wavelengths for NLPF measurements. Right part: NLPF signal from this complex probed at 840 nm and pumped between 825 and 860 nm, in comparison with the corresponding part of the absorption spectrum.

mediate case is shown in Fig. 2c. It is obvious that the intensity ratio of the two maxima is a good measure of the degree of inhomogeneity.

In all cases, the actual values of T_1 and T_2 can be obtained by fitting the experimental function to the appropriate lineshape function. For two level systems and the types of broadening discussed above, these bandshape formulas will be published in a separate paper.¹⁶ For three and four level systems with extremely inhomogeneous broadening these formulas can be found by Song *et al.*¹⁴ and Saikan and Sei.¹⁵

RESULTS AND DISCUSSION

With the isolated B800–850 complex of *Rb. sphaeroides* in LDAO, NLPF signals were measured at probe frequencies (ω_2) of 3.606×10^{14} Hz (832 nm), 3.571×10^{14} Hz (840 nm) and 3.488×10^{14} Hz (860 nm). The positions of these probe frequencies within the absorption spectrum of the complex are shown in Fig. 3. Also shown in this figure is the NLPF signal probed at 840 nm with ω_1 scanning between 825 and 860 nm. The shape of this signal is nearly symmetric with only a small hump on the long-wavelength side. It is noteworthy that a similar wide NLPF scanning at the probe wave-

lengths 832 nm and 860 nm gives neither a maximum nor even a significant hump at the maximum of the B850 absorption band. This means that the B850 component of the B800–850 antenna complex (FWHM = 405 cm^{-1}) is inhomogeneously broadened. Further results from the NLPF signal probed at 840 nm are a phase relaxation time $T_2 \approx 50$ fs and an energy relaxation time $T_1 \approx 1.5$ ps. From this a 210 cm^{-1} homogeneous width of the 840 nm absorbing subform of B850 follows.

For the NLPF signals probed at 832 nm and 860 nm, details of the central parts (experiment and simulation) are shown in Fig. 4; the wavelength spread is enlarged in comparison to Fig. 3. At 832 nm the determined T_1 and T_2 values are 5 ps and 260 fs, which gives a homogeneous width of 40 cm^{-1} for the subform centered at 832 nm. The corresponding values for the subform centered at 860 nm are 3.6 ps, 420 fs and 27 cm^{-1} .

Especially the 860 nm NLPF signal shows a lineshape asymmetry of the central part, which is different from the above-discussed asymmetry as a result of inhomogeneous broadening (intermediate case). We also observed a central part asymmetry at the other probe wavelengths by increasing the pump intensity. This calls for an extension of the model in the above-mentioned sense (*cp. Theoretical approach* above). This extension will especially qualify the conclusions from the central part of the NLPF lineshapes concerning energy relaxation and transfer processes within and between the antenna subforms. Therefore at this stage of investigation we defer any interpretations of the obtained T_1 value, which varies between 1.5 and 5 ps and does not belong to the fluorescence channel. The overall fluorescence lifetime of the B800–850 complex of about 1 ns¹⁷ is outside the transformed time range available with our present experimental setup (approx. 20 fs–50 ps).

It should be pointed out that the present results of inhomogeneous broadening of the B850 absorption band, the wavelength dependence of the homogeneous widths and the femtosecond phase relaxation time within the subforms of this antenna at room temperature are independent of this model extension.

The result of inhomogeneous broadening is in line with the conclusion by Zhang *et al.*⁵ that their finding of excitation wavelength dependence of LH2 → LH1 transfer time “strongly suggests that B850 is spectrally heterogeneous . . .” These authors underline that their data hardly allow a more sophisticated model. The need for more experimental data can be satisfied by NLPF investigations. In this first note on an application of this method in the field of photosynthesis, it is our aim to indicate the general content of information of NLPF, using the B800–850 complex as an example. To get a more detailed picture of the structure–function relationship with B850 further investigations are necessary (and are in progress, *e.g.*, also with chromatophores). On the basis of the present experimental data one can only imagine that the several B850 subforms represented in the distribution of homogeneous subbands over nearly the FWHM of the overall B850 absorption band reflect a size distribution of clusters of the B800–850 “minimal units” at room temperature. In this case the dephasing time depends on the cluster size. At low temperature, in line with results from exciton annihilation, one can assume that these minimal units are (com-

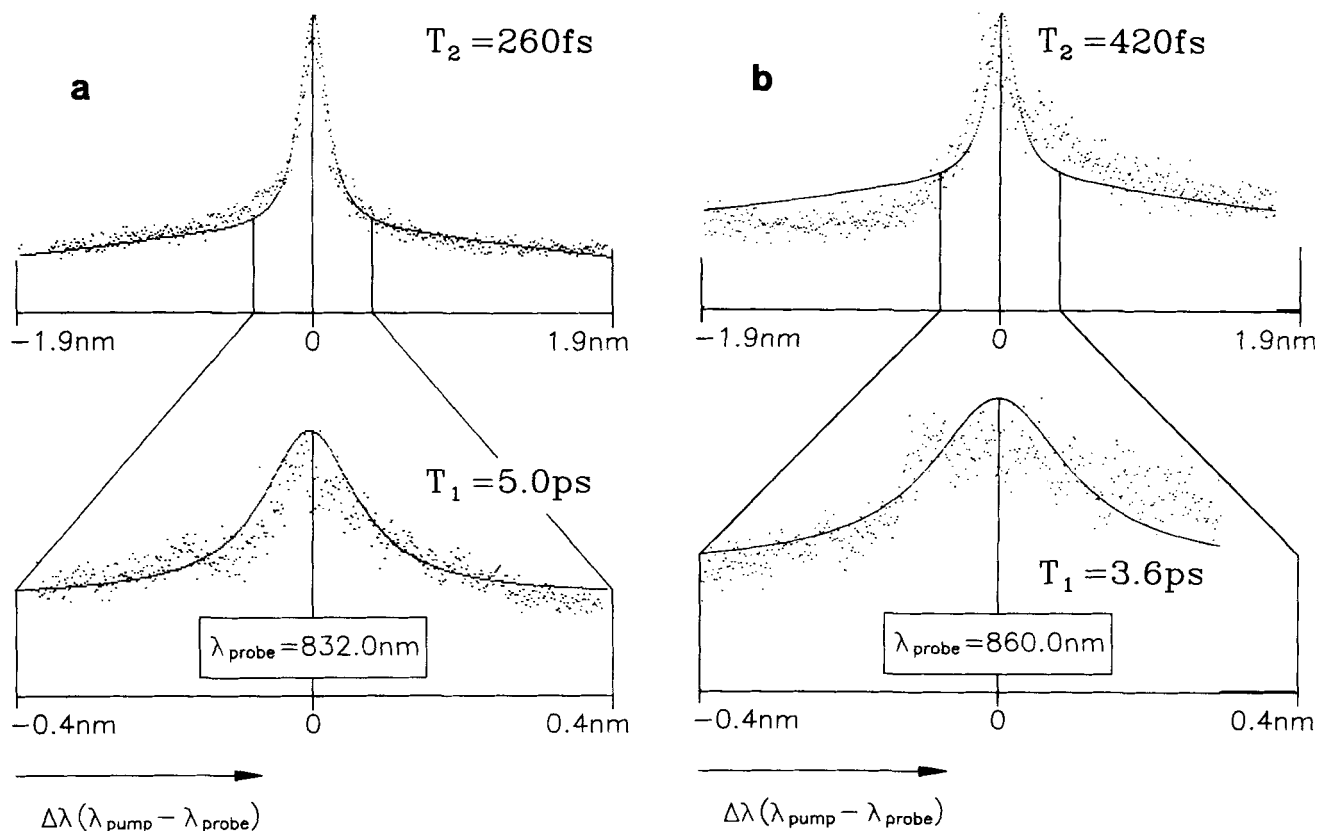


Figure 4. NLPF signals of B800–850 complex from *Rhodospira rubra* probed at 832 (a) and 860 nm (b). The lower trace is an expansion of the upper one, to give details of the wings and the central part, resp. Both parts have distinct but different weight in calculating T_1 and T_2 , resp. (cf. Theoretical approach).

pletely) uncoupled or they built small but unique clusters. This would explain the homogeneous broadening result of Small.⁷

CONCLUSIONS

Within the 850 nm absorption band of the isolated B800–850 antenna complex of *Rb. sphaeroides* distinct NLPF signals were obtained at room temperature. They indicate that the B850 component is inhomogeneously broadened and has much more substructure than found up to now by the B870 minor form. The homogeneous widths of the subforms vary between 210 cm^{-1} (at the B850 band center) and about 30 cm^{-1} (at the B850 band wings); the phase relaxation time of each subform is clearly in the subpicosecond range, varying from 50 fs to 420 fs. Also found is an energy relaxation channel in the range of some picoseconds.

A slightly pump-power-dependent weak asymmetry of all NLPF signals indicates contributions from processes between the subforms (energy transfer, spectral cross-relaxation) and/or exciton annihilation.

Acknowledgements—This work was supported by the Deutsche Forschungsgemeinschaft, Bonn (AZ Sche 140/13-1 and Le 729/1-1). M.B. is indebted to the Hans-Fischer-Gesellschaft, München, for a stipend. We thank the Bayrol company (München) for supplying the detergents. Stimulating discussions with Drs. J. Ehlert and E. Neef are gratefully acknowledged.

REFERENCES

1. Scheer, H. and S. Schneider (eds.) (1988) *Photosynthetic Light Harvesting Systems: Organization and Function*. W. DeGruyter, Berlin.
2. Scheer, H. (ed.) (1991) *Chlorophylls*. CRC Press, Boca Raton.
3. Hunter, C. N., H. Bergström, R. van Grondelle and V. Sundström (1990) Energy transfer dynamics in three light-harvesting mutants of *Rhodospira rubra*: a picosecond spectroscopy study. *Biochemistry* **29**, 3203–3207.
4. Visscher, K. J., M. Oskarsson, R. van Grondelle and V. Sundström (1993) Ultrafast energy transfer within the light-harvesting antenna of photosynthetic purple bacteria. *Photochem. Photobiol.* (In press)
5. Zhang, Fu Geng, R. van Grondelle and V. Sundström (1992) Pathways of energy flow through the light-harvesting antenna of the photosynthetic purple bacterium *Rhodospira rubra*. *Biophys. J.* **61**, 911–920.
6. Trautman, J. K., A. P. Shreve, C. A. Violette, H. A. Frank, T. G. Owens and A. C. Albrecht (1990) Femtosecond dynamics of energy transfer in B800–850 light-harvesting complexes of *Rhodospira rubra*. *Proc. Natl. Acad. Sci. USA* **87**, 215–219.
7. Reddy, N. R. S., R. J. Cogdell, L. Zaho and G. J. Small (1993) Nonphotochemical hole burning of the B800–B850 antenna complex of *Rhodospseudomonas acidophila*. *Photochem. Photobiol.* **57**, 35–39.
8. Nedbal, L. and V. Szöcs (1986) How long does excitonic motion in the photosynthetic unit remain coherent? *J. Theor. Biol.* **120**, 411–418.
9. Bittner, Th., J. Voigt, H. Kehrberg, J. Eckert and G. Renger (1991) Evidence of excited state absorption in PSII membrane fragments. *Photosynth. Res.* **28**, 131–137.

10. Bittner, Th., J. Voigt, K.-D. Irrgang and G. Renger (1993) Nonlinear laserspectroscopic investigations of the LHC of photosystem II. *Photochem. Photobiol.* **57**, 158–162.
11. Berthold, D. A., G. T. Babcock and C. F. Yocum (1981) A highly resolved, oxygen-evolving photosystem II preparation from spinach thylakoid membranes. *FEBS Lett.* **134**, 231–234.
12. Beese, D., R. Steiner, H. Scheer, A. Angerhofer, B. Robert and M. Lutz (1987) Chemically modified photosynthetic bacterial reaction centers: circular dichroism, Raman resonance, low temperature absorption fluorescence and ODMR spectra and polypeptide composition of borohydride treated reaction centers from *Rhodobacter sphaeroides* R26. *Photochem. Photobiol.* **46**, 293–304.
13. Laemmli, U. K. (1970) Cleavage of structural proteins during the assembly of the head of bacteriophage T4. *Nature* **227**, 680–685.
14. Song, J. J., J.-H. Lee and M. D. Levenson (1978) Picosecond relaxation measurements by polarization spectroscopy in condensed phases. *Phys. Rev. A* **17**, 1439–1447.
15. Saikan, S. and J. Sei (1983) Experimental studies of polarization spectroscopy in dye solutions. *J. Chem. Phys.* **79**, 4146–4153.
16. Mory, S. and E. Neef (1991) Content of information of nonlinear polarization spectroscopy. *Exp. Techn. Phys.* **39**, 385–388.
17. Bergström, H., V. Sundström, R. van Grondelle, A. Åkesson and T. Gillbro (1986) Energy transfer within the isolated light-harvesting B800–850 pigment–protein complex of *Rhodobacter sphaeroides*. *Biochim. Biophys. Acta* **852**, 279–287.